Published in final edited form as:
J Cogn Neurosci. 2006 March ; 18(3): 418–429. doi:10.1162/089892906775990552.

White Matter Changes Compromise Prefrontal Cortex Function in Healthy Elderly Individuals

Christine Wu Nordahl[1], **Charan Ranganath**[1], **Andrew P. Yonelinas**[1], **Charles DeCarli**[1], **Evan Fletcher**[1], and **William J. Jagust**[2]

[1]University of California at Davis

[2]University of California at Berkeley

Abstract

Changes in memory function in elderly individuals are often attributed to dysfunction of the prefrontal cortex (PFC). One mechanism for this dysfunction may be disruption of white matter tracts that connect the PFC with its anatomical targets. Here, we tested the hypothesis that white matter degeneration is associated with reduced prefrontal activation. We used white matter hyperintensities (WMH), a magnetic resonance imaging (MRI) finding associated with cerebrovascular disease in elderly individuals, as a marker for white matter degeneration. Specifically, we used structural MRI to quantify the extent of WMH in a group of cognitively normal elderly individuals and tested whether these measures were predictive of the magnitude of prefrontal activity (fMRI) observed during performance of an episodic retrieval task and a verbal working memory task.

We also examined the effects of WMH located in the dorsolateral frontal regions with the hypothesis that dorsal PFC WMH would be strongly associated with not only PFC function, but also with areas that are anatomically and functionally linked to the PFC in a task-dependent manner. Results showed that increases in both global and regional dorsal PFC WMH volume were associated with decreases in PFC activity. In addition, dorsal PFC WMH volume was associated with decreased activity in medial temporal and anterior cingulate regions during episodic retrieval and decreased activity in the posterior parietal and anterior cingulate cortex during working memory performance. These results suggest that disruption of white matter tracts, especially within the PFC, may be a mechanism for age-related changes in memory functioning.

INTRODUCTION

Evidence from behavioral and imaging studies suggests that aging is associated with prefrontal cortex (PFC) dysfunction (Cabeza, 2002; Logan, Sanders, Snyder, Morris, & Buckner, 2002; Rosen et al., 2002; Grady & Craik, 2000; Rypma & D'Esposito, 2000; Salat, Kaye, & Janowsky, 1999; Raz et al., 1997; West, 1996), but little is known about the underlying mechanisms. In this study, we test the hypothesis that deterioration of white matter tracts related to the presence of white matter hyperintensities (WMH) may be a mechanism for PFC dysfunction in elderly individuals. WMH are areas of high signal intensity on T2-weighted magnetic resonance imaging (MRI) scans, and the underlying pathology includes myelin loss, gliosis, and neuropil atrophy (Bronge, 2002). WMH are

Reprint requests should be sent to Christine Wu Nordahl, University of California-Davis, 2805 50th Street, Sacramento, CA 95817, or via crswu@ucdavis.edu.

The data reported in this experiment have been deposited in the fMRI Data Center (www.fmridc.org). The accession number is 2-2005-120FQ.

associated with small-vessel cerebrovascular disease and hypertension (DeCarli et al., 1995; Breteler, van Swieten, et al., 1994) and are commonly seen in cognitively normal elderly individuals (Wen & Sachdev, 2004; Soderlund, Nyberg, Adolfsson, Nilsson, & Launer, 2003).

Moreover, there is evidence that WMH are especially detrimental to the frontal lobes relative to the rest of the brain, with reports of selective decreases in *N*-acetylaspartate levels (a measure of neuronal viability) (Schuff et al., 2003) and resting glucose metabolism in the frontal lobes (Tullberg et al., 2004). There is also evidence that WMH are correlated with executive control deficits thought to arise from PFC dysfunction (Gunning-Dixon and Raz, 2000; DeCarli et al., 1995). Thus, we predicted that global WMH would be associated with a reduction in prefrontal function in elderly individuals during memory performance.

In addition, we were especially interested in the effects of regional WMH localized to dorsal PFC given the evidence suggesting that dorsal PFC may be disproportionately affected in aging (MacPherson, Phillips, & Della Sala, 2002; Rypma & D'Esposito, 2000). Dorsal PFC implements cognitive control processes that modulate activity in other areas during working memory and episodic memory tasks (Bunge, Burrows, & Wagner, 2004; Kondo et al., 2004; Ranganath, Johnson, & D'Esposito, 2003; Ranganath & Knight, 2003). We predicted that regional damage to white matter tracts within the dorsal PFC may disconnect the dorsal PFC from its targets and result in reduced recruitment in both the PFC and other brain regions that are functionally connected with dorsal PFC in a task-related manner.

We used structural and functional MRI to examine the relationship between WMH and PFC activity in a group of cognitively normal, elderly individuals during an episodic retrieval and a verbal working memory task, two tasks in which age-related changes in PFC activity have been observed (Tisserand & Jolles, 2003; Grady, 2000). We used structural images to quantify WMH and examined the effects of both global WMH and regional dorsal PFC WMH on task-related activity in PFC and in areas that are functionally related to PFC during episodic and working memory task performance. To investigate the effect of WMH on activity, we first identified regions of interest (ROIs) based on task-related activity and then correlated WMH volumes with the magnitude of activity within these regions. Specifically, we hypothesized that (1) global white matter degeneration would result in reduced activation in the PFC during each of the memory tasks and (2) regional white matter degeneration within dorsal PFC would result in reduced activation in PFC as well as in areas that interact with dorsal PFC in a task-specific manner. To control for the possibility that such correlations might be driven by nonspecific vascular or neural changes, we additionally examined visual cortex activation during performance of a simple visual task (under the assumption that neural activity during this task should not be correlated with WMH volume).

METHODS

Participants

Fifteen cognitively normal individuals (4 men/11 women) over the age of 65 (range, 66–86) participated in this study. All participants were recruited through the University of California-Davis Alzheimer's Disease Center (ADC), which maintains a pool of control subjects recruited either from the community through advertising or word of mouth, or through spouses or acquaintances of patients seen at the ADC. All participants received neurological examinations and neuropsychological evaluations and were adjudicated as normal at a multidisciplinary case conference, based upon all available clinical information. Neuropsychological testing included Mini Mental State Exam (MMSE), Wechsler Memory Scale-Revised (WMS-R) Logical Memory I and II, Memory Assessment Scales (MAS) List

Learning, Boston Naming, Block Design, and Digit Span. All subjects scored in the normal range on all administered neuropsychological tests (within 1.5 *SD* of age and education normative data). Demographic information and neuropsychological testing scores are presented in Table 1.

Importantly, individuals in this study were not preselected for presence or absence of WMH; they were selected on the basis of normal cognitive ability. In this respect, this sample is comparable to samples used in other functional neuroimaging studies of normal aging (e.g., Logan et al., 2002). Exclusion criteria included history of cortical stroke or other neurological disorder, clinical depression, major visual impairments, and any contraindications for MRI. Individuals with hypertension were not excluded from this study. Of the 15 subjects in this study, 7 individuals had hypertension and were taking antihypertensive medication. Systolic and diastolic blood pressure in individuals with (systolic: mean 139, *SD* 10.2; diastolic: mean 72, *SD* 5.0) and without hypertension (systolic: mean 140, *SD* 19.9; diastolic: mean 72, *SD* 11.1) did not differ (ps > .05). In addition, there were no significant differences between hypertensive and nonhypertensive subjects for global and dorsal PFC WMH volumes or in the magnitude of activation in any of the task-related regions reported on below.

Behavioral Task Paradigms

Episodic Memory Retrieval Task—The episodic memory test used in this study is a source memory task that has been shown to be sensitive to PFC and hippocampal function (Yonelinas, Hopfinger, Buonocore, Kroll, & Baynes, 2001). A schematic of this task is depicted in Figure 1A. During the study phase, participants viewed 36 pictures (18 red/18 green, self-paced) and were instructed to remember the color of the picture. Participants were instructed to verbalize an association between the object and the color in order to facilitate memory encoding. An immediate retrieval task was administered following the study phase. After a 1-hr delay, the delayed retrieval task was administered in the scanner. Subjects viewed the 36 pictures in black and white (2800 msec stimulus duration, 700 msec intertrial interval [ITI]) and made left/right button presses to indicate whether the picture had been red or green at study. Blocks of pictures alternated with blocks of a simple visual size-discrimination baseline task. This consisted of a central fixation cross with a shape (circles or squares) presented on either side of the cross. Participants were instructed to press a button to indicate which side (left or right) was larger. This baseline task was chosen because it required both visual encoding and a motor response, but no memory processes were engaged. Each run consisted of six blocks of each condition with six trials in each block.

Verbal Item Recognition Working Memory Task—This task has been shown to elicit dorsolateral PFC activations in older people when a high-load condition is used (Rypma & D'Esposito, 1999, 2000). In this study, we used two different load conditions, a four-letter version as the low load and a six-letter version as the high load. Separate functional MRI (fMRI) runs were used for each load. A schematic of the task is depicted in Figure 1B. Participants viewed the study letter set (2500 msec) followed by a short delay (1500 msec). A probe letter then appeared (2500 + 1500 msec ITI) and participants responded to indicate whether the probe letter matched any letter in the study set. The baseline condition consisted of a single letter in the study set, substantially reducing the memory load. Each run consisted of four blocks of each condition with four trials in each block.

Visual Sensory Control Task—We used this task as a control to assess whether vascular abnormalities associated with WMH fundamentally alter the fMRI BOLD signal. The task consisted of alternating blocks of a flickering checkerboard (16 sec) followed by

fixation (16 sec). Each run consisted of eight blocks of each condition. Participants were instructed to fixate on the screen for the duration of the run.

Procedures

All participants gave informed consent to participate in the study. After completing an MRI screening questionnaire, subjects were familiarized with the behavioral tasks in a practice session outside of the scanner. Participants were then fitted with scanner-compatible eyeglasses if necessary.

Each scanning session consisted of collection of structural images followed by six functional scans: the episodic retrieval task, two runs each of the low- and high-load working memory task (for a total of four runs of the working memory task), followed by the visual sensory task. The order of the structural and functional scans was the same for every participant. Stimuli were presented using Presentation v.7.0 (nbs.neuro-bs.com), projected onto a screen located at the end of the MRI gantry, and viewed by means of a mirror inset in the head coil. Participants made left-/right-hand responses using two fiber-optic button press boxes, one in each hand. Due to technical difficulties, data from one run of the high load working memory task is missing for one subject and data from the visual task is missing for two subjects.

MRI Data Acquisition

All MRI data for each subject were acquired in a single session on a 1.5T GE Signa scanner at the UC Davis Imaging Research Center. Functional imaging was performed using a gradient echo-planar imaging (EPI) sequence (TR = 2000, TE = 50, FOV = 24 cm, 64 × 64 matrix, 22 axial slices, 5 mm thick). Structural imaging sequences included a fluid-attenuated inversion recovery (FLAIR) (FOV = 24 cm, 48 slices, 3 mm thick) sequence for WMH quantification, a high-resolution 3-D coronal T1-weighted spoiled gradient-echo (SPGR) and a PD/T2-weighted fast spin-echo sequence collected in the same plane as the functional images.

WMH Segmentation and Quantification

Segmentation of WMH volumes was performed on the FLAIR images as described previously (DeCarli, Murphy, Teichberg, Campbell, & Sobering, 1996; DeCarli et al., 1992; Murphy, DeCarli, Schapiro, Rapoport, & Horwitz, 1992). In brief, initial reorientation of the 3-D volume images was performed so that brain regions were accurately delineated using common internal landmarks (Murphy et al., 1993, 1996). Prior to segmentation, nonbrain elements were manually removed from the image by operator-guided tracing of the dura matter within the cranial vault and image intensity nonuniformity correction was applied (DeCarli et al., 1996). Our method of image segmentation rests on the assumption that, within a given 2-D image, image pixel intensities for each tissue type (such as cerebral spinal fluid [CSF] and brain matter, or gray matter and white matter) have their own population distribution that differs, but possibly overlaps with that of the other tissue types.

CSF–brain matter segmentation was obtained by mathematically modeling the pixel intensity distributions from each image using Gaussian normal distributions as previously described (DeCarli et al., 1992). The optimal segmentation threshold was defined as the intersection of the CSF modeled distribution with the brain matter modeled distribution (DeCarli et al., 1992). After image segmentation of brain from CSF was performed, the pixel intensity histogram of the brain-only FLAIR image was modeled as a lognormal distribution, and pixel intensities three and one-half standard deviations above the mean were considered WMH (DeCarli et al., 1995).

Each subject's FLAIR and segmented WMH image were then linearly aligned to his or her high-resolution T1 image, and the T1 image was spatially normalized to a minimal deformation target (MDT) (see below for details on spatial normalization and the MDT). Each subject's T1 to MDT warping parameters were then applied to their segmented WMH image to bring it into MDT space. To measure global WMH volume, total WMH volume was normalized to the MDT volume for each subject. The data were then log transformed because the distribution of WMH volume/brain volume was positively skewed.

The dorsal PFC region was then delineated on the MDT as described previously (Tullberg et al., 2004). In brief, a ray-casting program was used to create different ROIs. The dorsal PFC region was created by casting three rays: (1) one ray along the axis of the anterior and posterior commissure, (2) a second ray parallel to the first, but at the superior boundary of the callosal body, and (3) a third ray running perpendicular from ray 1 at the point of the anterior commissure. The dorsal PFC region was delineated as the volume resulting from the intersection of rays 2 and 3. The resulting region included the superior frontal gyrus and the superior portion of the middle frontal gyrus (BA 8 and 9 and the superior portion of BA 10 and 46). Dorsal PFC WMH volumes were calculated from the underlying white matter of this region by counting the number of voxels on each subject's segmented WMH image that fell within this region. Volumes for left and right hemispheres were added together to determine the regional dorsal PFC WMH volume for each individual.

fMRI Data Preprocessing and Spatial Normalization

Functional imaging data were realigned in SPM99 and spatially normalized using in-house, atlas-based, high-dimensional nonlinear warping procedure (cubic B-splines) and spatially smoothed with an 8-mm full width half maximum Gaussian filter. Due to structural brain changes, such as atrophy, that are characteristic of aging brains (Salat et al., 2004; Good et al., 2001), we did not use the standard MNI template (an average of MRIs from 152 young subjects) as a target for spatial normalization. Instead, we derived an MDT image, an anatomically detailed synthetic image to be used as a target for spatial normalization. By using the MDT as a template, we were able to minimize the total deformations that result when warping the template onto each subject of that data set. Moreover, the nonlinear warping techniques used here allow for independent adjustment of local matches, resulting in preservation of anatomical detail. Accordingly, this procedure maximized our sensitivity to detect activations in across-subject analyses.

The MDT image was derived as follows: First, an arbitrarily selected image from the study was used as a preliminary target and warped onto each of the subject images. The average deformation of all warps from the target to each subject was computed. Next, the preliminary target was deformed by this average deformation to produce the minimal deformation template. The subject images were again normalized, this time to the minimal deformation target.

The warping method was a multigrid application of cubic B-splines. A grid of equally spaced control points enables locally independent warps to be constructed in small subvolumes defined by cubes having control points as vertices. These result in a matching of fine anatomical details. Each data voxel in the target and subject image is contained within a $4 \times 4 \times 4$ cube of such control points, and its position is defined by a sum of tensor products of B-spline basis functions (third order polynomials) together with the positions of these control points. The third-order polynomial basis functions guarantee that the local warps are smoothly joined at the boundaries of the cubes. By changing one or more of these grid points, the location of the voxel can be adjusted. Because this adjustment is dependent on local parameters only (the locations of the neighboring 64 grid points), we can obtain a finer anatomical match than is achievable using linear or nonlinear globally parameterized

transformations. The multigrid approach refers to using control point grids of successively finer mesh. We used 32-, 16-, 8-, 4-, and 2-mm control point separations in succession.

Normalization of the EPI images posed a challenge because of their lack of anatomical detail and also an inherent nonlinear field distortion when compared with the anatomical images. To overcome these difficulties we first linearly aligned (12-parameter) each subject's mean EPI with their coplanar T2-weighted image, which afforded better gross boundary contrasts than the T1. The T2-weighted image was, in turn, coregistered with the T1. We then used a coarse-grid (32 mm) spline warp to adjust the EPI field distortion.

fMRI Data Analyses

For each task, each individual's spatially normalized data were modeled using a modified general linear model (GLM) as implemented in VoxBo (www.voxbo.org). Covariates representing the contrast of activity during each task relative to its respective baseline condition were constructed by convolving a boxcar function with a hemodynamic response function. Additional nuisance covariates modeled motion-correlated signals, global signal changes (orthogonalized with respect to the design matrix) (Desjardins, Kiehl, & Liddle, 2001), inter-scan baseline shifts, and an intercept. Each GLM also included filters to remove frequencies below 0.02 Hz and above 0.25 Hz.

Next, a random-effects analysis was used to identify areas of activation observed across the entire group of subjects. In this analysis, images of parameter estimates were derived for each contrast for each subject and entered into a second-level, one-sample t test in which the mean estimate across participants at each voxel was tested against zero. Significant regions of activation were identified using an uncorrected one-tailed threshold of $p < .001$ and a minimum cluster size of 10 contiguous voxels.

To examine correlations between WMH volume and PFC activation, we first defined prefrontal ROIs based on the group-averaged statistical parametric map (SPM) by selecting all contiguous suprathreshold voxels in anatomically constrained areas, the middle frontal gyrus (BA 9/46) for dorsal PFC and the inferior frontal gyrus (BA 44/45/47) for ventral PFC. Each ROI was then used as a mask and applied to single-subject data. Parameter estimates, indexing activation during each task relative to its baseline condition, were averaged over the entire mask and then entered into second-level analyses with subjects as a random variable. Pearson correlation coefficients were derived to identify the relationship between WMH volume and averaged parameter estimates for each ROI. A Fisher's r to z transformation was carried out to determine whether the correlation coefficient was significantly different from zero.

We also defined task-related ROIs of activity outside of the PFC to explore the possibility that dorsal PFC WMH volume may also be associated with activity in other regions that are functionally connected. The additional ROIs examined were based on previous functional imaging studies as well as studies of anatomical connectivity and are discussed separately for each task. The ROIs were delineated based on the group-averaged activations for each task, and mean parameter estimates were correlated with dorsal PFC WMH volumes.

RESULTS

WMH Volumes

Consistent with previous studies (e.g., de Leeuw et al., 2001; Breteler, van Amerongen, et al., 1994), we found a positive correlation between age and global WMH volume ($R = .590$, $p = .02$). However, age was not significantly correlated with brain activity in any of the PFC

ROIs examined. Thus, age confounds could not account for any of the observed relationships between WMH and PFC activity.

In order to compare the extent of WMH in this sample relative to the general population, we examined how subjects in this sample compared to percentiles from a larger sample of nondemented individuals from a population-based study (Wu et al., 2002). We found that 87% of subjects in the current study had WMH volumes less than the 75th percentile of the larger study. Thus, the majority of subjects in this study had minimal to moderate WMH volumes. Individual examples of the extent of WMH are depicted in Figure 2.

Behavioral Results

Episodic Memory Task—An immediate retrieval task was administered after the study phase (mean accuracy: 0.82, $SD = .08$), and after a delay of 1 hr, a delayed retrieval task was administered during scanning (mean accuracy: 0.75, $SD = .12$). Performance was not significantly correlated with age (immediate: $R = -.322$, $p = .25$; delayed: $R = -.241$, $p = .39$). The correlations between performance and global WMH volume were as follows: immediate; $R = -.394$, $p = .15$; delayed; $R = -.494$, $p = .06$, and correlations between performance and dorsal PFC WMH volume were as follows: immediate; $R = -.555$, $p = .03$; delayed; $R = -.477$, $p = .07$.

Verbal Working Memory Task—Accuracy was very high for both low- and high-load conditions. Mean accuracy was 0.94 ($SD = .05$) for the low-load condition and 0.88 ($SD = .07$) for the high-load condition. Performance was not significantly correlated with age (low load: $R = -.463$; $p = .08$; high load $R = -.280$, $p = .32$). Correlations between performance and global WMH volume were as follows: low load; $R = -.421$, $p = .12$; high load; $R = -.469$, $p = .08$, and correlations between performance and dorsal PFC WMH were as follows: low load; $R = -.144$, $p = .62$; high load; $R = -.419$, $p = .12$.

fMRI Results

Episodic Memory Task

Group activations: Figure 3A depicts group-averaged activations during the episodic memory task. This analysis revealed significant regions of activation in the right middle frontal gyrus (BA 9), right inferior frontal gyrus (BA 44/45/47), anterior cingulate gyrus (BA 32), posterior cingulate gyrus (BA 23/29/31), bilateral medial temporal lobes (hippocampus, BA 28/36), and right parietal cortex (BA 7/40) (for a complete summary of significant activations, see Table 2).

Global WMH and PFC activity: Global WMH volume was marginally negatively correlated with right ventral PFC activity ($R = -.453$, $p = .09$). Global WMH volume was not significantly correlated with right or left dorsal PFC activity ($R = -.403$, $p = .13$; $R = -.309$, $p = .27$) or left ventral PFC ($R = -.373$, $p = .17$) activity.

Dorsal PFC WMH and brain activity: To test the prediction that dorsal PFC WMH may be associated with decreased recruitment of PFC and other brain regions that are functionally related to PFC, we first correlated measures of dorsal PFC WMH volume with activity in the PFC ROIs. As shown in Table 3, dorsal PFC WMH volume was strongly negatively correlated with activations in dorsal and left ventral PFC, with a similar trend evident in right ventral PFC.

We then correlated dorsal PFC WMH volume with parameter estimates indexing activation in other cortical regions that are recruited during episodic retrieval. Previous functional imaging studies suggest that in addition to dorsal and ventral PFC activity, episodic retrieval

is also associated with medial temporal lobe (MTL), anterior cingulate (BA 24/32), posterior cingulate (BA 23/29/30), and posterior parietal (BA 40) cortex activity (see Tisserand & Jolles, 2003; Buckner & Wheeler, 2001; Cabeza & Nyberg, 2000). Consistent with these studies, we observed activations in these areas and delineated additional ROIs based on the group-averaged activation maps. As seen in Table 3, dorsal PFC WMH volumes were also negatively correlated with activation in bilateral MTL, anterior cingulate cortex (BA 32), and right parietal cortex (BA 7/40) activity. To a lesser extent, there was also an association with posterior cingulate cortex activity (BA 23/29/31).

Verbal Working Memory

Group activations: Group activations for the high-load condition are depicted in Figure 3B. This analysis revealed significant activations in the bilateral middle frontal gyrus (BA 9/46), bilateral inferior frontal gyrus (BA 44/45), anterior cingulate gyrus (BA 32), and bilateral parietal cortex (BA 7) (for a complete summary of significant activations, see Table 4). For the low-load condition, we again observed significant group activations in bilateral middle frontal gyrus (BA 9/46), bilateral inferior frontal gyrus (BA 44/45), anterior cingulate gyrus (BA2 4/32), and bilateral parietal cortex (BA 7/40) (for complete summary of activations, see Table 5).

Global WMH and PFC activity: As shown in Figure 4, for the high-load condition, global WMH volume was negatively correlated with left ($R = -.654$, $p = .007$) and right ($R = -.607$, $p = .015$) dorsal PFC activity. In addition, global WMH volume was negatively correlated with ventral PFC activity, but these effects were not statistically significant (right: $R = -.438$, $p = .104$; left: $R = -.479$, $p = .071$). For the low-load condition, the pattern of results is similar to the results for the high-load condition, albeit with less robust correlations (dorsal PFC: left $R = -.447$, $p = .096$; right $R = -.491$ $p = .063$; ventral PFC: left $R = -.362$, $p = .189$, right $R = -.501$, $p = .057$).

Dorsal PFC WMH and brain activity: As shown in Table 3, dorsal PFC WMH volume was significantly negatively correlated with bilateral dorsal and ventral PFC activations. Outside of the PFC, we delineated additional ROIs based on the group-averaged activations in areas that have been consistently identified in imaging studies of verbal working memory. Specifically, we were interested in the anterior cingulate cortex (BA 24/32) and posterior parietal cortex (BA 7/40), two areas that are commonly activated during working memory tasks (see Smith & Jonides, 1999). Also shown in Table 3, dorsal PFC WMH volume was also significantly negatively correlated with the anterior cingulate and left parietal cortex. A similar correlation was observed in the right parietal cortex, but was not statistically significant. For the low-load condition, again, the pattern of results is similar, but the magnitude of the correlations was slightly lower than for the high-load condition.

Visual Sensory Control Task—To control for the possibility that nonspecific vascular changes associated with WMH fundamentally alter the BOLD response, we examined the effect of WMH volume on visual cortex activation. The purpose of using a simple sensory task was to minimize any cognitive component that may alter brain activity. Thus, any relationship between visual cortex activity and WMH volume would presumably be explained by differences in hemodynamic response. As expected, group analyses revealed robust bilateral activations in the primary visual cortex (BA 17). An ROI was delineated and magnitude of activity was correlated with WMH volume. There were no significant correlations between either global WMH volume or dorsal PFC WMH volume and activity in this region (all ps > .39).

DISCUSSION

The frontal aging hypothesis suggests that age-related cognitive decline is a consequence of selective degeneration of the prefrontal cortex (Tisserand & Jolles, 2003; West, 1996), but the biological mechanism underlying these changes is unknown. In this study, we tested the hypothesis that disruption of white matter integrity associated with cerebrovascular disease may play a role in PFC dysfunction during episodic memory retrieval and verbal working memory in a group of cognitively normal elderly individuals. Our results show that PFC function is sensitive to both global WMH as well as regional dorsal PFC WMH. In addition, regional dorsal PFC WMH are associated with other brain areas that are functionally connected to PFC in a task-dependent manner. There was no relationship between WMH and visual cortex activity during a visual sensory task, suggesting that these correlations could not be attributed to global alterations in neurovascular coupling.

WMH are extremely prevalent in elderly individuals, and there is evidence that WMH have a selective effect on the frontal lobes, with reports of selective decreases in *N*-acetylaspartate levels (Schuff et al., 2003) and resting glucose metabolism in the frontal lobes (Tullberg et al., 2004; DeCarli et al., 1995). There is also some evidence from diffusion tensor imaging studies that selective deterioration of frontal white matter tracts occurs in older individuals (Head et al., 2004; O'Sullivan et al., 2001). Consistent with these findings, we found that increased global WMH volume was associated with decreased bilateral dorsal PFC activity during a working memory task and modestly associated with right ventral PFC during episodic retrieval, suggesting that diffuse disconnection of white matter tracts throughout the brain may be a mechanism for disruption of PFC function in aging. Moreover, we found that regional WMH in dorsal PFC was strongly associated with decreased PFC activity during both episodic retrieval and working memory performance. These results suggest that WMH located in dorsal PFC may be especially detrimental to PFC function in aging.

We additionally predicted that regional WMH within dorsal PFC would be associated with dysfunction in other brain regions that are functionally and anatomically linked to the PFC. For the episodic memory task, we were specifically interested in the circuitry between PFC and the MTL. One recent study reported an age-related change in hippocampal–prefrontal connectivity during an episodic encoding task (Grady, McIntosh, & Craik, 2003). Our results showed that an increase in dorsal PFC WMH volume was associated with decrease in bilateral MTL activity, suggesting that connectivity between these areas may be disrupted.

For the working memory task, we were specifically interested in the possibility that disruption of the prefrontal–parietal connections known to be involved in working memory processes (Chafee & Goldman-Rakic, 2000; Selemon & Goldman-Rakic, 1988) may occur. Indeed, we found that dorsal PFC WMH volume was also associated with bilateral parietal activation during the working memory task, suggesting that connectivity between the PFC and posterior parietal cortex may be disrupted.

Interestingly, we observed a strong association between anterior cingulate cortex activation and dorsal PFC WMH in both the episodic retrieval and verbal working memory tests. The anterior cingulate is associated with cognitive control processes, especially those involved in conflict resolution (Carter, Botvinick, & Cohen, 1999). Recent evidence suggests that functional connectivity between the anterior cingulate cortex and PFC may be involved in successful working memory performance (Kondo et al., 2004) and difficult episodic retrieval conditions (Bunge et al., 2004). Our results suggest that disruption of this circuit may underlie the age-related deficits in working memory and episodic retrieval.

These results are consistent with our hypothesis that disruption of white matter tracts within dorsal PFC results in decreased recruitment of both PFC and functionally linked targets in other brain regions. However, we cannot rule out the possibility that decreased recruitment in the other brain regions results from a more generalized effect of global damage to white matter tracts affecting a larger network of regions that underlie memory function rather than specific disruption of white matter tracts within dorsal PFC. Additional studies specifically addressing connectivity, perhaps using diffusion tensor imaging in conjunction with functional MRI will allow for investigation into these functional and anatomical circuits with more specificity.

WMH, Aging, and Cognition

Psychological data suggest that elderly individuals are selectively impaired on tasks that tap prefrontal cortex function, including working memory tasks (MacPherson et al., 2002) as well as standard neuropsychological tests such as the Wisconsin Card Sorting Test (WCST) (MacPherson et al., 2002; Craik, Morris, Morris, & Loewen, 1990). In a parallel line of research, several studies have shown that WMH are also correlated with deficits on the WCST and other neuropsychological tests that are sensitive to prefrontal function (Gunning-Dixon & Raz, 2000; DeCarli et al., 1995).

In this study, there were modest associations between WMH volumes and performance on episodic retrieval and working memory tasks. It is important to emphasize two factors when considering these results. First, the present study was not designed to elicit large intersubject variability in performance. Our objective was to assess activation while holding behavioral performance at a high accuracy level to reduce the possibility for performance to confound any activation results. Second, with 15 subjects, assuming an alpha = 0.05 and a two-sided test, we have 80% power to detect a correlation of $R = .62$. Although this level of statistical power is commensurate with most published fMRI studies, we emphasize that a failure to find a significant correlation must be interpreted cautiously. It is possible, and even likely, that either increasing the sample size or using more demanding versions of these tasks would elicit greater behavioral deficits, and that these deficits would be associated with WMH volume. Indeed, in a recent study of elderly individuals with mild cognitive impairment, a subgroup with extensive WMH showed significant behavioral deficits on the memory tasks used in this study (Nordahl, Ranganath, Yonelinas, DeCarli, & Jagust, 2005).

WMH, Cerebrovascular Disease, and Aging Studies

WMH are associated with various cerebrovascular risk factors such as hypertension, atherosclerosis, smoking, and diabetes (Bronge, 2002), and epidemiological surveys suggest that the prevalence of WMH in elderly individuals is close to 100% (Wen & Sachdev, 2004; Soderlund et al., 2003; de Leeuw et al., 2001). Given that WMH and the associated risk factors, especially hypertension, are so prevalent and may play a role in producing cognitive impairment (Raz, Rodrigue, & Acker, 2003), understanding the role that they play in the aging brain is crucial. Importantly, the presence of WMH can often go undetected because obvious clinical symptoms are lacking. In light of the current evidence suggesting that WMH are associated with compromised PFC function, careful examination of subject inclusion for normal aging studies is necessary in order to differentiate the potential pathological influence of WMH from true age-related changes.

Conclusion

In summary, we found that disruption of white matter integrity may be one mechanism for PFC dysfunction commonly seen in elderly individuals. Available evidence suggests that WMH are associated with behavioral deficits in executive function and may selectively decrease frontal lobe function. Accordingly, our data show that increasing WMH volume

was associated with decreased PFC recruitment during episodic and working memory tasks in cognitively normal elderly individuals. This has several important implications for the field of aging. Moreover, WMH are associated with cerebrovascular disease, which is both preventable and amenable to intervention by changes in lifestyle or medications. It is therefore possible that some age-related cognitive decline could be treated or even prevented.

Acknowledgments

This project was supported by NIH grants P30 AG10129, MH59352, and R01 AG021028 and in part by funding from the NIMH predoctoral National Research Service Award MH-065082 awarded to CWN.

References

Breteler MM, van Amerongen NM, van Swieten JC, Claus JJ, Grobbee DE, van Gijn J, Hofman A, van Harskamp F. Cognitive correlates of ventricular enlargement and cerebral white matter lesions on magnetic resonance imaging. The Rotterdam Study. Stroke. 1994; 25:1109–1115. [PubMed: 8202966]

Breteler MM, van Swieten JC, Bots ML, Grobbee DE, Claus JJ, van den Hout JH, van Harskamp F, Tanghe HL, de Jong PT, van Gijn J. Cerebral white matter lesions, vascular risk factors, and cognitive function in a population-based study: The Rotterdam Study. Neurology. 1994; 44:1246–1252. [PubMed: 8035924]

Bronge L. Magnetic resonance imaging in dementia. A study of brain white matter changes. Acta Radiologica, Supplementum. 2002; 43:1–32. [PubMed: 12108231]

Buckner RL, Wheeler ME. The cognitive neuroscience of remembering. Nature Reviews Neuroscience. 2001; 2:624–634.

Bunge SA, Burrows B, Wagner AD. Prefrontal and hippocampal contributions to visual associative recognition: Interactions between cognitive control and episodic retrieval. Brain and Cognition. 2004; 56:141–152. [PubMed: 15518931]

Cabeza R. Hemispheric asymmetry reduction in older adults: The HAROLD model. Psychology and Aging. 2002; 17:85–100. [PubMed: 11931290]

Cabeza R, Nyberg L. Imaging cognition II: An empirical review of 275 PET and fMRI studies. Journal of Cognitive Neuroscience. 2000; 12:1–47. [PubMed: 10769304]

Carter CS, Botvinick MM, Cohen JD. The contribution of the anterior cingulate cortex to executive processes in cognition. Reviews in the Neurosciences. 1999; 10:49–57. [PubMed: 10356991]

Chafee MV, Goldman-Rakic PS. Inactivation of parietal and prefrontal cortex reveals interdependence of neural activity during memory-guided saccades. Journal of Neurophysiology. 2000; 83:1550–1566. [PubMed: 10712479]

Craik FI, Morris LW, Morris RG, Loewen ER. Relations between source amnesia and frontal lobe functioning in older adults. Psychology and Aging. 1990; 5:148–151. [PubMed: 2317296]

de Leeuw FE, de Groot JC, Achten E, Oudkerk M, Ramos LM, Heijboer R, Hofman A, Jolles J, van Gijn J, Breteler MM. Prevalence of cerebral white matter lesions in elderly people: A population based magnetic resonance imaging study. The Rotterdam Scan Study. Journal of Neurology, Neurosurgery, and Psychiatry. 2001; 70:9–14.

DeCarli C, Maisog J, Murphy DG, Teichberg D, Rapoport SI, Horwitz B. Method for quantification of brain, ventricular, and subarachnoid CSF volumes from MR images. Journal of Computer Assisted Tomography. 1992; 16:274–284. [PubMed: 1545026]

DeCarli C, Murphy DG, Teichberg D, Campbell G, Sobering GS. Local histogram correction of MRI spatially dependent image pixel intensity nonuniformity. Journal of Magnetic Resonance Imaging. 1996; 6:519–528. [PubMed: 8724419]

DeCarli C, Murphy DG, Tranh M, Grady CL, Haxby JV, Gillette JA, Salerno JA, Gonzales-Aviles A, Horwitz B, Rapoport SI. The effect of white matter hyperintensity volume on brain structure, cognitive performance, and cerebral metabolism of glucose in 51 healthy adults. Neurology. 1995; 45:2077–2084. [PubMed: 7501162]

Desjardins AE, Kiehl KA, Liddle PF. Removal of confounding effects of global signal in functional MRI analyses. Neuroimage. 2001; 13:751–758. [PubMed: 11305902]

Good CD, Johnsrude IS, Ashburner J, Henson RN, Friston KJ, Frackowiak RS. A voxel-based morphometric study of ageing in 465 normal adult human brains. Neuroimage. 2001; 14:21–36. [PubMed: 11525331]

Grady CL. Functional brain imaging and age-related changes in cognition. Biological Psychology. 2000; 54:259–281. [PubMed: 11035226]

Grady CL, Craik FI. Changes in memory processing with age. Current Opinion in Neurobiology. 2000; 10:224–231. [PubMed: 10753795]

Grady CL, McIntosh AR, Craik FI. Age-related differences in the functional connectivity of the hippocampus during memory encoding. Hippocampus. 2003; 13:572–586. [PubMed: 12921348]

Gunning-Dixon FM, Raz N. The cognitive correlates of white matter abnormalities in normal aging: A quantitative review. Neuropsychology. 2000; 14:224–232. [PubMed: 10791862]

Head D, Buckner RL, Shimony JS, Williams LE, Akbudak E, Conturo TE, McAvoy M, Morris JC, Snyder AZ. Differential vulnerability of anterior white matter in nondemented aging with minimal acceleration in dementia of the Alzheimer type: Evidence from diffusion tensor imaging. Cerebral Cortex. 2004; 14:410–423. [PubMed: 15028645]

Kondo H, Morishita M, Osaka N, Osaka M, Fukuyama H, Shibasaki H. Functional roles of the cingulo-frontal network in performance on working memory. Neuroimage. 2004; 21:2–14. [PubMed: 14741637]

Logan JM, Sanders AL, Snyder AZ, Morris JC, Buckner RL. Under-recruitment and nonselective recruitment: Dissociable neural mechanisms associated with aging. Neuron. 2002; 33:827–840. [PubMed: 11879658]

MacPherson SE, Phillips LH, Della Sala S. Age, executive function and social decision making: A dorsolateral prefrontal theory of cognitive aging. Psychology and Aging. 2002; 14:598–609. [PubMed: 12507357]

Murphy DG, DeCarli C, Daly E, Haxby JV, Allen G, White BJ, McIntosh AR, Powell CM, Horwitz B, Rapoport SI, Schapiro MB. X-chromosome effects on female brain: A magnetic resonance imaging study of Turner's syndrome. Lancet. 1993; 342:1197–1200. [PubMed: 7901528]

Murphy DG, DeCarli C, McIntosh AR, Daly E, Mentis MJ, Pietrini P, Szczepanik J, Schapiro MB, Grady CL, Horwitz B, Rapoport SI. Sex differences in human brain morphometry and metabolism: An in vivo quantitative magnetic resonance imaging and positron emission tomography study on the effect of aging. Archives of General Psychiatry. 1996; 53:585–594. [PubMed: 8660125]

Murphy DG, DeCarli C, Schapiro MB, Rapoport SI, Horwitz B. Age-related differences in volumes of subcortical nuclei, brain matter, and cerebrospinal fluid in healthy men as measured with magnetic resonance imaging. Archives of Neurology. 1992; 49:839–845. [PubMed: 1343082]

Nordahl CW, Ranganath C, Yonelinas AP, DeCarli C, Jagust WJ. Different mechanisms of episodic memory failure in mild cognitive impairment. Neuropsychologia. 2005; 43:1688–1697. [PubMed: 16009250]

O'Sullivan M, Jones DK, Summers PE, Morris RG, Williams SC, Markus HS. Evidence for cortical "disconnection" as a mechanism of age-related cognitive decline. Neurology. 2001; 57:632–638. [PubMed: 11524471]

Ranganath C, Johnson MK, D'Esposito M. Prefrontal activity associated with working memory and episodic long-term memory. Neuropsychologia. 2003; 41:378–389. [PubMed: 12457762]

Ranganath, C.; Knight, R. Prefrontal cortex and episodic memory: Integrating findings from neuropscyhology and functional brain imaging. In: Amanda Parker, TB.; Wilding, E., editors. Memory encoding and retrieval: A cognitive neuroscience perspective. Hove, UK: Psychology Press; 2003.

Raz N, Gunning FM, Head D, Dupuis JH, McQuain J, Briggs SD, Loken WJ, Thornton AE, Acker JD. Selective aging of the human cerebral cortex observed in vivo: Differential vulnerability of the prefrontal gray matter. Cerebral Cortex. 1997; 7:268–282. [PubMed: 9143446]

Raz N, Rodrigue KM, Acker JD. Hypertension and the brain: Vulnerability of the prefrontal regions and executive functions. Behavioral Neuroscience. 2003; 117:1169–1180. [PubMed: 14674838]

Rosen AC, Prull MW, O'Hara R, Race EA, Desmond JE, Glover GH, Yesavage JA, Gabrieli JD. Variable effects of aging on frontal lobe contributions to memory. NeuroReport. 2002; 13:2425–2428. [PubMed: 12499842]

Rypma B, D'Esposito M. The roles of prefrontal brain regions in components of working memory: Effects of memory load and individual differences. Proceedings of the National Academy of Sciences, USA. 1999; 96:6558–6563.

Rypma B, D'Esposito M. Isolating the neural mechanisms of age-related changes in human working memory. Nature Neuroscience. 2000; 3:509–515.

Salat DH, Buckner RL, Snyder AZ, Greve DN, Desikan RS, Busa E, Morris JC, Dale AM, Fischl B. Thinning of the cerebral cortex in aging. Cerebral Cortex. 2004; 14:721–730. [PubMed: 15054051]

Salat DH, Kaye JA, Janowsky JS. Prefrontal gray and white matter volumes in healthy aging and Alzheimer disease. Archives of Neurology. 1999; 56:338–344. [PubMed: 10190825]

Schuff N, Capizzano AA, Du AT, Amend DL, O'Neill J, Norman D, Jagust WJ, Chui HC, Kramer JH, Reed BR, Miller BL, Yaffe K, Weiner MW. Different patterns of *N*-acetylaspartate loss in subcortical ischemic vascular dementia and AD. Neurology. 2003; 61:358–364. [PubMed: 12913198]

Selemon LD, Goldman-Rakic PS. Common cortical and subcortical targets of the dorsolateral prefrontal and posterior parietal cortices in the rhesus monkey: Evidence for a distributed neural network subserving spatially guided behavior. Journal of Neuroscience. 1988; 8:4049–4068. [PubMed: 2846794]

Smith EE, Jonides J. Storage and executive processes in the frontal lobes. Science. 1999; 283:1657–1661. [PubMed: 10073923]

Soderlund H, Nyberg L, Adolfsson R, Nilsson LG, Launer LJ. High prevalence of white matter hyperintensities in normal aging: Relation to blood pressure and cognition. Cortex. 2003; 39:1093–1105. [PubMed: 14584568]

Tisserand DJ, Jolles J. On the involvement of prefrontal networks in cognitive ageing. Cortex. 2003; 39:1107–1128. [PubMed: 14584569]

Tullberg M, Fletcher E, DeCarli C, Mungas D, Reed BR, Harvey DJ, Weiner MW, Chui HC, Jagust WJ. White matter lesions impair frontal lobe function regardless of their location. Neurology. 2004; 63:246. [PubMed: 15277616]

Wen W, Sachdev P. The topography of white matter hyperintensities on brain MRI in healthy 60- to 64-year-old individuals. Neuroimage. 2004; 22:144–154. [PubMed: 15110004]

West RL. An application of prefrontal cortex function theory to cognitive aging. Psychological Bulletin. 1996; 120:272–292. [PubMed: 8831298]

Wu CC, Mungas D, Petkov CI, Eberling JL, Zrelak PA, Buonocore MH, Brunberg JA, Haan MN, Jagust WJ. Brain structure and cognition in a community sample of elderly Latinos. Neurology. 2002; 59:383–391. [PubMed: 12177372]

Yonelinas AP, Hopfinger JB, Buonocore MH, Kroll NE, Baynes K. Hippocampal, parahippocampal and occipital–temporal contributions to associative and item recognition memory: An fMRI study. NeuroReport. 2001; 12:359–363. [PubMed: 11209950]

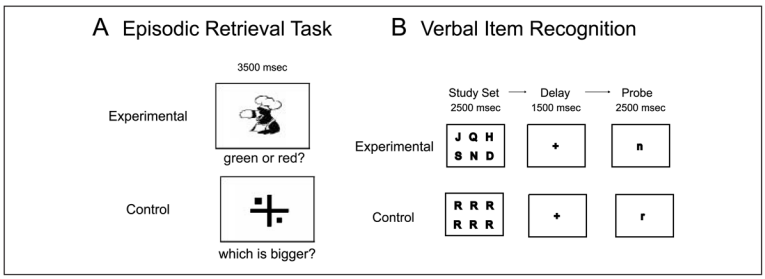

Figure 1.

Behavioral tasks. (A) Episodic retrieval task. Participants first studied 36 objects (18 red/18 green). After a 1-hr delay, during scanning, participants viewed all 36 pictures again in black and white during the experimental blocks and indicated the color at study with a left or right button press. The control condition was a visual size-discrimination task. (B) The high-load working memory task is depicted here. The low-load condition was the same except that the study set contained four letters.

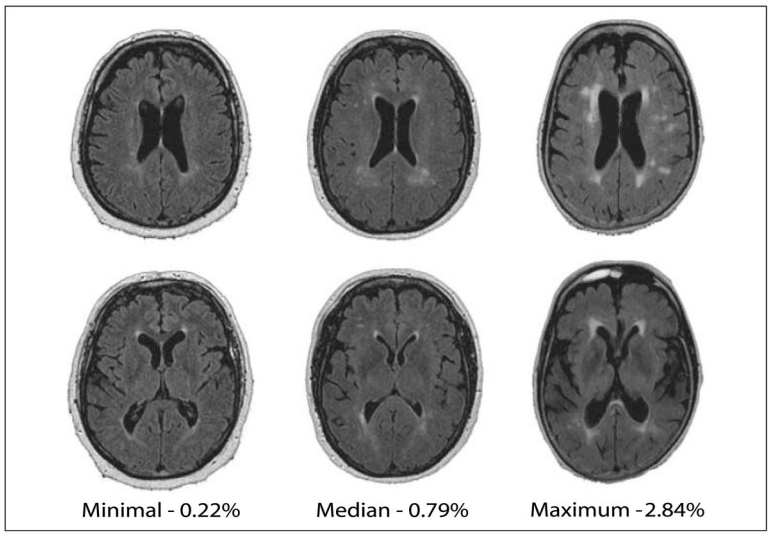

Figure 2.
Examples of the extent of WMH from individual subjects in this study. WMH load is expressed as percent of total cranial volume.

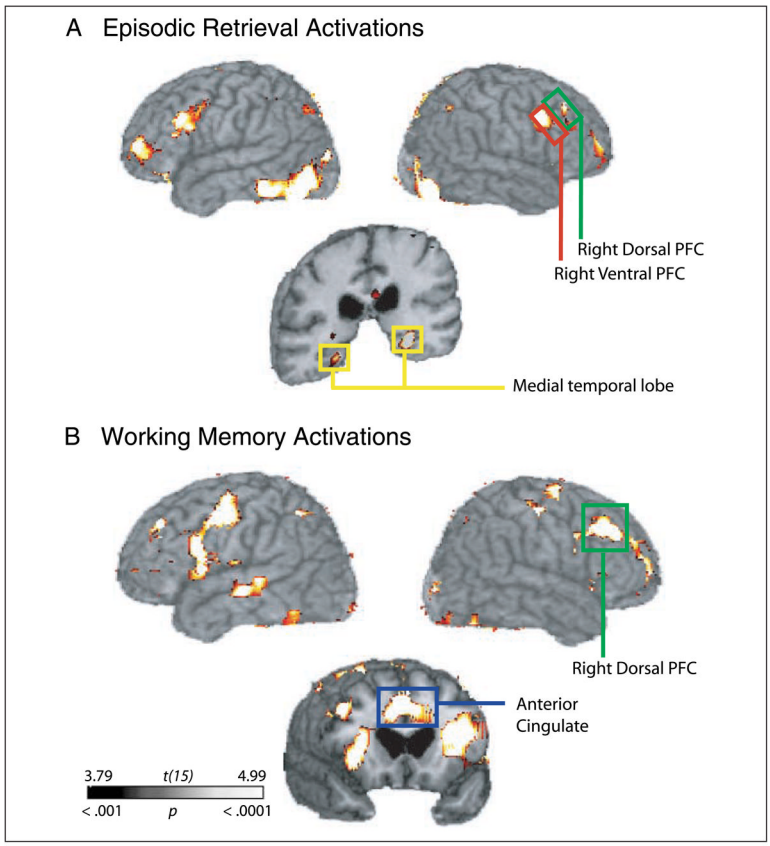

Figure 3.
Group-averaged activations. (A) Episodic retrieval task and (B) High-load working memory task ($p < .001$ uncorrected, 10 voxel cluster threshold).

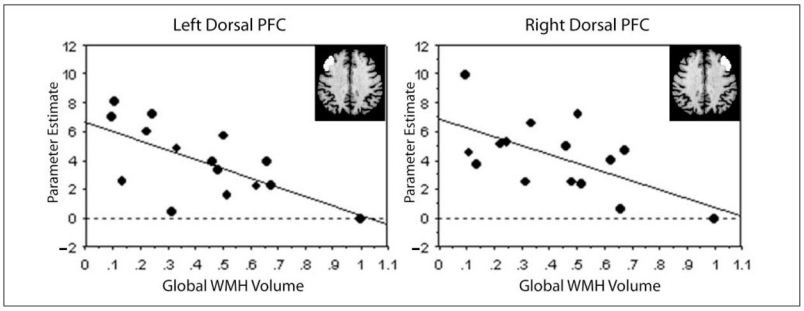

Figure 4.

Global WMH volume is negatively correlated with activity in the dorsal prefrontal cortex during the high-load working memory task. Parameter estimates, indexing magnitude of activity during episodic retrieval relative to baseline, were averaged over each ROI for each subject. Global WMH volume is expressed as the log transform of total WMH load.

Table 1

Demographic Information, Neuropsychological Testing Scores, and WMH Volumes

Age	78.7 (6.06)
Education	15.3 (2.29)
MMSE	29.6 (.51)
Digit Span	14.5 (3.1)
Block Design	25.1 (7.5)
Boston Naming	55.2 (4.5)
Logical Memory I	25.8 (5.9)
Logical Memory II	23.3 (5.3)
MAS-Delayed Recall	10.8 (.84)
Total WMH volume	0.875% (.73)
Dorsal PFC WMH volume	0.390% (.53)

Where applicable, data are expressed as mean (*SD*). Total WMH is expressed as percent of total cranial volume. Regional WMH is expressed as percent of total regional volume. MMSE =Mini Mental State Exam; MAS = Memory Assessment Scales; WMH = white matter hyperintensity; PFC = prefrontal cortex.

Table 2

Activations for Episodic Retrieval Task

Region	BA	x	y	z	t(15)
R. middle frontal gyrus	9/46	44	42	24	4.69
R. inferior frontal gyrus	47	34	22	−6	6.21
R. posterior inferior frontal gyrus	44	38	8	30	4.77
R. middle frontal gyrus	10	24	52	−8	5.98
L. middle frontal gyrus	9/46	−36	28	2	8.29
L. inferior frontal gyrus	45	−46	28	12	6.10
L. medial frontal gyrus	6	−2	8	62	4.94
L. precentral gyrus	4	−40	−4	34	7.92
L. precentral gyrus	6	−48	4	18	5.75
L. middle frontal gyrus	10	−28	48	−2	6.98
R. cingulate gyrus	32	10	24	26	6.45
L. cingulate gyrus	32	−6	20	34	8.71
L. posterior cingulate gyrus	23	−10	−54	12	4.77
R. posterior cingulate gyrus	29	12	−44	10	4.06
L. and R. posterior cingulate gyrus	31/23	0	−34	34	5.37
L. hippocampus		−28	−32	−10	7.93
R. hippocampus		24	−32	−10	5.34
R. parahippocampal gyrus	28/36	26	−24	−18	3.97
R. superior parietal lobule	7/40	36	−52	52	5.17
R. inferior parietal lobule	40	32	−50	30	5.56
R. middle occipital gyrus	19	48	−76	−4	11.26
L. middle occipital gyrus	19	−42	−74	−8	7.38

Coordinates are transformed to a standard stereotactic space (MNI) to facilitate comparison with other imaging studies.

R = right; L = left.

Table 3

Correlation Coefficients for Dorsal PFC WMH Volumes and Activity in Task-dependent Regions of Interest

	Episodic Retrieval	High-Load Working Memory	Low-Load Working Memory
L. dorsal PFC	−.563*	−.688**	−.565*
R. dorsal PFC	−.568*	−.661**	−.562*
L. ventral PFC	−.602*	−.723**	−.626*
R. ventral PFC	−.473	−.575	−.348
L. MTL	−.512	–	–
R. MTL	−.653**	–	–
ACC	−.618*	−.682**	−.556*
PCC	−.490	–	–
L. parietal	−.393	−.599*	−.559*
R. parietal	−.540*	−.424	−.584*

PFC = prefrontal cortex; MTL = medial temporal lobe; ACC = anterior cingulate cortex; PCC = posterior cingulate cortex; L = left; R = right.

* $p < .05$.

** $p < .01$.

Table 4

Activations for Verbal Item Recognition Task at High-load Working Memory Task

Region	BA	x	y	z	t(15)
R. middle frontal gyrus	9/46	44	32	30	8.98
R. middle frontal gyrus	10	32	56	4	6.47
R. middle frontal gyrus	6	26	2	58	7.21
R. inferior frontal gyrus	45	32	28	4	8.06
R. precentral gyrus	4	48	−10	50	7.27
L. middle frontal gyrus	9/46	−36	38	10	8.21
L. middle frontal gyrus	10	−38	54	−4	4.67
L. middle frontal gyrus	6	−38	−6	40	7.65
L. inferior frontal gyrus	44	−58	8	4	5.70
L. precentral gyrus	6	−24	−56	52	8.08
R. insula		30	16	22	10.33
L. insula		−30	0	18	10.38
R. anterior cingulate gyrus	32	4	22	36	8.48
L. anterior cingulate gyrus	32	−4	18	36	7.40
R. inferior parietal lobule	7	28	−61	40	8.67
L. inferior parietal lobule	7	−22	−62	46	7.82
L. superior parietal lobule	7	−12	−62	50	7.43
R. middle occipital gyrus	18	20	−84	0	7.99
L. middle occipital gyrus	19	−24	−80	20	8.49
R. fusiform gyrus	37	46	−42	−12	5.48
L. fusiform gyrus	37	−44	−40	−14	9.39

Coordinates are transformed to a standard stereotactic space (MNI) to facilitate comparison with other imaging studies.

R = right; L = left.

Table 5

Activations for Verbal Item Recognition Task at Low-load Working Memory Task

Region	BA	x	y	z	t(15)
R. middle frontal gyrus	9/46	36	36	24	4.52
R. inferior frontal gyrus	44	36	8	24	5.61
R. precentral gyrus	6	36	4	24	5.61
L. middle frontal gyrus	9/46	−42	30	16	4.98
L. middle frontal gyrus	6	−38	−4	56	6.48
L. inferior frontal gyrus	45	−52	20	24	4.88
L. precentral gyrus	4	−46	−4	46	6.22
R. anterior cingulate gyrus	24/32	2	12	24	6.37
L. anterior cingulate gyrus	24/32	−4	8	34	5.96
R. inferior parietal lobule	7	34	−60	50	6.00
L. inferior parietal lobule	7	−22	−62	44	5.25
L. inferior parietal lobule	40	−42	−44	34	4.97
R. fusiform gyrus	19	34	−62	−26	4.91
R. middle occipital gyrus	18	30	−86	4	5.27
L. middle occipital gyrus	18	−30	−84	−10	4.65
R. thalamus		18	−2	−6	5.47

Coordinates are transformed to a standard stereotactic space (MNI) to facilitate comparison with other imaging studies.